New method for detecting fast neutrino flavor conversions in core-collapse supernova models with two-moment neutrino transport

Hiroki Nagakura[*]
Department of Astrophysical Sciences, Princeton University, 4 Ivy Lane, Princeton, New Jersey 08544, USA

Lucas Johns[†]
Department of Physics, University of California, Berkeley, California 94720, USA

(Received 8 June 2021; accepted 11 August 2021; published 8 September 2021)

Fast-pairwise neutrino oscillations potentially affect many aspects of core-collapse supernovae (CCSNe): the explosion mechanism, neutrino signals, and nucleosynthesis in the ejecta. This particular mode of collective neutrino oscillations has a deep connection to the angular structure of neutrinos in momentum space; for instance, the appearance of electron-neutrino lepton number (ELN) angular crossings in momentum space is a good indicator of the occurrence of flavor conversions. However, many multidimensional CCSN simulations are carried out with approximate neutrino transport (such as two-moment methods), which limits access to the angular distributions of neutrinos, i.e., inhibits ELN-crossing searches. In this paper, we develop a new method of searching for ELN crossing in these CCSN simulations. The required data is the zeroth and first angular moments of neutrinos and the matter profile, all of which are available in CCSN models with the two-moment method. One of the novelties of our new method is the use of a ray-tracing neutrino transport to determine ELNs in the direction of the stellar center. It is designed to compensate for shortcomings of the crossing searches with only two angular moments. We assess the capability of the method by carrying out a detailed comparison with results of full Boltzmann neutrino transport in 1D and 2D CCSN models. We find that the ray-tracing neutrino transport improves the accuracy of crossing searches; indeed, the appearance/disappearance of the crossings is accurately detected even in the region of forward-peaked angular distributions. The new method is computationally cheap and has the benefit of efficient parallelization; hence, it will be useful for ELN-crossing searches in any CCSN models that employ two-moment neutrino transport.

DOI: 10.1103/PhysRevD.104.063014

I. INTRODUCTION

Neutrinos have been recognized as one of the key players in core-collapse supernovae (CCSNe). It has been suggested that the energy, momentum, and lepton number exchange between matter and neutrinos sways the destiny of the collapsing star; for instance, neutrino heating in the post-shock flows revitalizes the stagnated shock wave, i.e., triggering the onset of the explosion (for recent reviews see, e.g., Refs. [1–4]). The nuclear composition of the ejecta is also dictated by neutrino-matter interactions, which sensitively depend on the energy spectrum of all flavors of neutrinos [5–14]. From an observational point of view, neutrino signals offer a diagnostic for CCSN dynamics [15–23]. They are detectable for nearby CCSNe by currently operating and planned terrestrial neutrino detectors (for recent reviews see, e.g., Refs. [24,25]). Coincident neutrino detections by multiple observatories with different reaction channels will shed light on flavor-dependent features of neutrinos, which would provide precious information on deciphering CCSN dynamics and subsequent neutron star or black hole formation [26–28]. Hence, the accurate determination of the neutrino radiation field is one of the fundamental tasks towards comprehensive understanding of death of massive stellar collapse.

A complete description of neutrino dynamics requires solving multidimensional (multi-D), multiflavor, multienergy, and multiangle neutrino transport equations. Assuming that neutrino flavor conversions are suppressed by high matter density [29], the transport equation can be given by a Boltzmann equation. Recently, multi-D CCSN models with full Boltzmann neutrino transport have become available, which allows us to access the 3D features of neutrino momentum space [30–33]. On the other hand, it has been recognized that the assumption is not valid if instabilities of flavor conversion are turned on by neutrino

[*]hirokin@astro.princeton.edu
[†]NASA Einstein Fellow.
ljohns@berkeley.edu

self-interactions [34], which are also known as collective neutrino oscillations. In this case, the transport equation needs to be altered from the Boltzmann equations [35–42]. The mean-field quantum kinetic equation seems to be the simplest extension while also capturing some essential features of flavor conversions. However, it involves technical difficulties in the numerical treatments, since the self-interactions are highly nonlinear phenomena and there is a striking disparity in both spatial and time scales between flavor conversions and CCSN dynamics. These practical issues have been obstackled for the detailed study of flavor conversions (but see the recent efforts in, e.g., Refs. [43–55]). For these reasons, the actual impact of flavor conversions on CCSN dynamics and the observational consequences still remain very elusive.

This paper is devoted to providing a new method for analyzing *fast-pairwise neutrino oscillation* [56]. It is one of the collective neutrino oscillation modes and potentially generates strong and rapid flavor conversions. The linear analysis and some relevant numerical studies suggest that the electron-neutrino lepton number (ELN) angular crossings[1] trigger the flavor conversion (see, e.g., Refs. [55,62–66]). Thus, searching ELN crossings in the neutrino data of theoretical CCSN models is the most straightforward way to judge whether fast flavor conversion occurs in the CCSN environment.

Detailed angular information about each flavor of neutrino is mandatory to carry out ELN-crossing searches. However, the high computational burden of CCSN simulations with multiangle neutrino transport impedes progress. Although there are several multi-D CCSN models with full Boltzmann neutrino transport at present [67–71] (hereafter, Ref. [69] is denoted as N19), they are nowhere near enough to scrutinize the progenitor- and time-dependent features. More importantly, there are no available 3D radiation-hydrodynamic simulations with Boltzmann neutrino transport in the phase of interest for fast flavor conversions.[2] On the other hand, we can run dozens of 3D simulations covering the post-bounce phase up to ~ 1 s, if we use approximations in the computation of neutrino transport. The most popular method is a two-moment approximation, in which the zeroth and first angular moments are solved with a closure relation for higher moments [73–79]. The angular degrees of freedom in neutrino momentum space are integrated out in this method, i.e., the number of dimensions in the neutrino transport is only four (three in space and one in neutrino energy). This approximation alleviates the computational cost substantially; consequently, two-moment methods have become standard in 3D CCSN models [80–92]. Hence, it is worth considering how we utilize CCSN models with two-moment neutrino transport for the analysis of fast flavor conversions.

In the last few years, great efforts have been devoted to developing surrogate methods to study fast flavor conversions based on neutrino data of two-moment neutrino transport. The *zero mode search* may be the simplest one. This method takes advantage of the following properties of flavor conversion. The stability with respect to a homogeneous ($k = 0$) mode in the corotating frame can be determined only from an inequality equation that is written as a function of the zeroth, first, and second angular moments [93,94], indicating that the simulations with two-moment neutrino transport provide sufficient information on the analysis. Another surrogate method was also proposed in Ref. [95] (hereafter referred to as the *polynomial method*). Similar to the zero mode search, it uses only a few angular moments of neutrinos. On the other hand, this method accesses the angular structure of ELN by using a polynomial function of directional cosines of the neutrino flight direction. In the method, ELN crossings are identified by the sign of the angular integrated quantities (see Ref. [95] for more details). This method was applied to neutrino data of 1D [61] and 3D [96] CCSN simulations, and the authors found positive signs of the occurrence of ELN crossings in these models.

Although these pioneering works paved the way to analyze fast flavor conversions in CCSN models with two-moment neutrino transport, their accuracy and validity are another matter. Let us point out that both methods need to rely on closure relations, which cannot be given accurately in the semitransparent region of neutrinos by analytic prescriptions (see, e.g., Refs. [30,31,33,97]). Next, we found some cases where unstable modes appear at $k \neq 0$, whereas the $k = 0$ mode is stable (see, e.g., Fig. 3 in N19), indicating that the zero mode search potentially leads to misjudgment. For the polynomial method, on the other hand, the authors applied the method in the region with forward-peaked neutrino angular distributions. However, the higher-rank angular moments of neutrinos were completely neglected in the method. This would lead to misjudgments of ELN crossings, since the role of the high angular moments in characterizing the full angular

[1]In this paper, we only focus on the angular distributions of electron-type neutrinos (ν_e) and their antipartners ($\bar{\nu}_e$); equivalently, we assume that all heavy leptonic neutrinos have identical energy spectra and angular distributions. However, this is in general not true since the cross sections of neutrino-matter interactions depend on flavors, and the difference may be outstanding if on-shell muons appear in a CCSN core [57–59]. We refer readers to Refs. [60,61] for possible influences of the heavy leptonic neutrinos in fast flavor conversion.

[2]A 3D CCSN simulation with full Boltzmann neutrino transport was performed in Ref. [33]. However, it is only up to a time $\lesssim$20 ms after bounce. In this phase, no fast-pairwise flavor conversions are expected due to the strong suppression of $\bar{\nu}_e$ emissions (see Ref. [72] for more details). We also note that the ELN search based on 3D full Boltzmann CCSN models in Refs. [67,70] is not under fully consistent treatments. They solved neutrino transport on top of a fixed matter background, which was extracted from other CCSN simulations, until the field reached a steady state.

distribution becomes more important with growing forward-peaked angular distributions.

Motivated by these concerns, we have recently scrutinized the capabilities of both methods [98,99] (hereafter, Ref. [99] is denoted as N21). As predicted, we found that the angular distributions of incoming neutrinos are much less constrained by the zeroth and first angular moments than those of outgoing ones. The insensitivity of incoming neutrinos to the low angular moments is an intrinsic limitation of moment methods; in other words, it is a common issue among all ELN-crossing searches. For these reasons, we conclude that ELN-crossing searches that only use a few angular moments are not accurate, and they are only valid in the optically thick region.

This paper is devoted to getting rid of the limitation; indeed, our new method presented in this paper is capable of precisely detecting ELN crossings in the region of forward-peaked angular distributions. The essence of our idea is as follows. Let us first point out that the angular distributions of outgoing neutrinos can be reconstructed very well using the method developed in N21. In other words, if we can overcome the shortage of reconstructing angular distributions of incoming neutrinos, the accuracy of ELN-crossing searches would be substantially improved. We tackle the issue by employing a ray-tracing method. One may wonder if the ray-tracing method is computationally expensive similar as full Boltzmann neutrino transport. Although it is true, we can substantially reduce the computational cost for the following reasons. In previous studies, we have witnessed that the number of ELN crossings in the momentum space of neutrinos is usually one in a CCSN environment (see, e.g., Ref. [67] and N19). In this case, the signs of ELNs at $\mu = 1$ and $\mu = -1$, where μ denotes the radial directional cosines for neutrino flight directions with respect to the radial basis, are opposite to each other. In other words, the appearance of ELN crossings can be judged by checking the signs of ELNs at $\mu = 1$ and $\mu = -1$. Since we can accurately reconstruct the ELN at $\mu = 1$ using our new method of N21, the ray-tracing neutrino transport along the direction of $\mu = -1$ provides crucial information on judging ELN crossings. It should also be mentioned that, even in (spatially) 3D CCSN models, the total number of rays along which we need to solve the transport equation is $N_\theta \times N_\phi \times N_\varepsilon$, where N_θ, N_ϕ, N_ε denote the number of grid points of the lateral direction, azimuthal direction, and neutrino energy, respectively. Since all rays can be solved independently (see Sec. II for more details),[3] our method is suitable for parallel computations. This also reduces the required computational time for ELN-crossing searches.

There is also another reason why the ray-tracing method is suited for our new method. As is well known, one of the disadvantages of the ray-tracing method is the treatment of scatterings. To evaluate the inscattering contributions, information on the full angular distributions of neutrinos is mandatory in general, i.e., the transport equations along different rays are coupled. Since this requires iterative computations in general, transport simulations become computationally expensive. In our method, however, we can overcome this difficulty by using the reconstructed angular distributions of neutrinos from the zeroth and first moments.[4] This breaks the coupling of transport equations and no iterative procedures are involved. This property is an important benefit in our hybrid approach.

This paper is organized as follows. We first describe the essence of our new method in Sec. II. In Sec. III we assess the capability (and validity) of our new ELN-crossing search by comparing results of 1D and 2D CCSN simulations with full Boltzmann neutrino transport. Finally, we summarize our conclusions in Sec. IV. We use the metric signature $-+++$. Unless otherwise stated, we work in units with $c = G = \hbar = 1$, where G and $\hbar$ denote the gravitational constant and the reduced Planck constant, respectively.

II. METHODS

In our method, we start by reconstructing the angular distributions of neutrinos from the zeroth and first angular moments obtained from CCSN simulations with two-moment neutrino transport. Although it is, in general, impossible to retrieve accurate angular distributions only from such lower angular moments, our previous study in N21 demonstrated a reasonable reconstruction. This success is based on the fact that there are some characteristic properties in the neutrino radiation field of CCSNe; indeed, some interesting correlations emerge between low angular moments and the full distributions in neutrino data of the CCSN model with Boltzmann neutrino transport [100]. Taking advantage of the correlations, we determine some free parameters of a fitting function, for which the shape of the angular distributions is determined solely from a flux factor (κ) (see N21 for more details).[5] The capability of our method was assessed by using a recent 2D CCSN model[6] [32]. The demonstration illustrated the strength of our

[3]If we include neutrino-matter interactions of nonisoenergetic processes, the energy coupling is inevitable in the ray-tracing method. However, the nonisoenergetic scatterings are subdominant in a CCSN core; hence, we can safely neglect the contribution.

[4]As we shall discuss in Sec. II, we consider isoenergetic scatterings in this paper. The reaction rate can be written in terms of the zeroth and first angular moments. Hence, the reconstruction of full angular distributions is not always necessary to compute the inscattering contribution.

[5]The resultant fitting parameters are publicly available at https://www.astro.princeton.edu/hirokin/scripts/data.html.

[6]In multi-D CCSN models, the angular distributions of neutrinos are no longer axisymmetric in momentum space. Hence, we employed the azimuthal-average angular distributions of neutrinos in the neutrino data of 2D CCSN simulations.

method: the angular distributions of outgoing neutrinos can be accurately reconstructed regardless of κ. In the present study, we take advantage of this merit: the ELN at $\mu = 1$ (along the outgoing radial direction) is computed from the reconstructed distribution of ν_e and $\bar{\nu}_e$ (see below for more details). We also underlined a weakness of the method: it is not capable of determining angular distributions of incoming neutrinos for large κ, i.e., forward-peaked distributions. In this paper, we use a ray-trace method to compensate for this shortcoming. We refer readers to N21 for more details of our reconstruction method.

In the present method, we judge appearances of ELN crossing by comparing the signs of ELNs at $\mu = 1$ (outgoing) and $\mu = -1$ (incoming) angular points. The ray-tracing transport is in charge of computing the ELN at $\mu = -1$. If the signs of the ELNs are opposite to each other, this indicates the appearance of ELN crossing. On the other hand, if the signs are the same, we cannot make a robust judgement in general, since this corresponds to the case of either no crossings or an even number of crossings. This shortcoming can be improved by solving radiation transport equations for different angles, i.e., we need to increase the number of rays. However, the computational cost would be increased accordingly, which reduces the merit (cheap computation) of our new method. It should be pointed out that recent ELN-crossing searches based on CCSN models with full Boltzmann neutrino transport suggest that the number of ELN crossings is usually one in a CCSN core (see, e.g., N19). Therefore, we judge no ELN crossings if the sign is the same in this study, although we need to keep in mind the uncertainty.

In our ray-tracing computations, we impose several approximations: the space-time is flat; no fluid-velocity dependences are taken into account; neutrino radiation fields have already settled into a steady state. Under these assumptions, the transport equation can be written as an ordinary differential equation,

$$-\frac{d}{dr} f_{\rm in}(\varepsilon, r) = \left(\frac{\delta f_{\rm in}}{\delta t}\right)_{\rm col} (\varepsilon, r), \tag{1}$$

where ε, r, and t denote the energy of neutrinos, radius, and time, respectively. $f_{\rm in}$ represents the distribution function of neutrinos (f) in the direction of $\mu = -1$. The right-hand side of Eq. (1) represents the neutrino-matter interactions. If the reaction rates employed in CCSN simulations with two-moment neutrino transport are available in the output data, they may be directly used for this ray-tracing computation. Otherwise, we need to take the fluid data from the output, and then compute each reaction rate by a post-processing manner. Although it is recommended to employ the same weak interaction rates used in CCSN simulations, this may result in increasing the computational cost. For the usability purpose, we recommend using a minimum but essential set of weak interactions in the post-shock region of a CCSN core: electron captures by free protons (and the inverse reaction), positron captures by free neutrons (and the inverse reaction), scatterings to nucleons, and coherent ones to heavy nuclei.[7] One may wonder if thermal processes such as electron-positron pairs and nucleon-nucleon bremsstrahlung processes need to be taken into account. However, those reactions are important only in optically thick regions where the angular distributions of neutrinos (including incoming directions) can be well reconstructed (see N21). This indicates that our ray-tracing method is not necessary in this region; hence, we stop the ray-tracing computation before entering the optically thick region (see below for more details). Therefore, the ignorance of the thermal processes in the ray-tracing method is a reasonable approximation. Indeed, we will show that ELN-crossing searches under these approximations lead to consistent judgement to the result of full Boltzmann neutrino transport.

We remark on the computation of scatterings in our method, since it generally requires a special attention for ray-tracing transport. The collision term of scatterings in Eq. (1) can be written as a sum of inscattering and outscattering components. They can be written as

$$\left(\frac{\delta f_{\rm in}}{\delta t}\right)_{\rm inscat} = \frac{(\varepsilon)^2}{(2\pi)^3} \int d\Omega' R_{\rm scat}(\Omega') f(\Omega'),$$
$$\left(\frac{\delta f_{\rm in}}{\delta t}\right)_{\rm outscat} = -\frac{(\varepsilon)^2}{(2\pi)^3} f_{\rm in} \int d\Omega' R_{\rm scat}(\Omega'), \tag{2}$$

where $R_{\rm scat}$ denotes the scattering kernel (which can be computed from fluid data). We refer readers to Ref. [102] for more general expressions. As shown in Eq. (2), the outscattering component can be computed without any problems, since the required information on the neutrino distribution function is only $f_{\rm in}$, which is obtained from the transport equation along the same radial ray. On the other hand, the inscattering component depends on f in different angular directions, indicating that the transport equation cannot be closed by the single ray. In this study, we employ f reconstructed from the method of N21 from the zeroth and first angular moments in the computation of inscattering rates.[8]

We solve Eq. (1) from the outer boundary of te CCSN simulation to the radially inward direction. As we have already pointed out, ray-tracing neutrino transport is necessary only in the optically thin region where neutrino

[7]We compute these reaction rates following Ref. [101].

[8]We note that the angular dependence of the scattering kernel $R_{\rm scat}$ for both the nucleon and heavy nuclei is up to the first order of directional cosine of the scattering angle unless the energy exchange is taken into account, indicating that the angular integration with f can be written in terms of zeroth and first angular moments. Hence, it is also possible to evaluate the inscattering component by directly using the moment data extracted from CCSN simulations.

angular distributions are forward peaked. Thus, we connect the obtained $f_{\rm in}$ to that reconstructed from zeroth and first moments; the details of the procedure are as follows. We first prepare two threshold flux factors: κ_1 and κ_2 ($\kappa_1 < \kappa_2$). In the region where $\kappa < \kappa_1$ (optically thick region), $f_{\rm in}$ is determined from the reconstructed distribution ($f_{\rm in}^{\rm reco}$). In the region where $\kappa > \kappa_2$, we employ the solution of ray-tracing neutrino transport ($f_{\rm in}^{\rm RT}$). In the intermediate region ($\kappa_1 < \kappa < \kappa_2$), we determine $f_{\rm in}$ by mixing the two solutions. More specifically, it is obtained as

$$f_{\rm in} = q(\kappa) f_{\rm in}^{\rm RT} + (1 - q(\kappa)) f_{\rm in}^{\rm reco}(\kappa), \tag{3}$$

where

$$q(\kappa) = \frac{\kappa - \kappa_1}{\kappa_2 - \kappa_1}. \tag{4}$$

As shown above, ray-tracing neutrino transport is necessary in the region where $\kappa > \kappa_1$.

The two parameters κ_1 and κ_2 are determined following the result of N21. We find that $f_{\rm in}^{\rm reco}$ agrees reasonably well with the results of Boltzmann neutrino transport at $\kappa \lesssim 0.4$, whereas it deviates from the original at $\kappa \gtrsim 0.5$; hence, we adopt $\kappa_1 = 0.4$ and $\kappa_2 = 0.5$ in this study. Since the neutrino-matter interactions sensitively depend on neutrino energy, the matching region should also be varied with neutrino energy. Our method is capable of capturing such an energy-dependent feature (as long as the neutrino data provided by CCSN simulations is energy dependent). Although ELN-crossing searches are done for the energy-integrated quantities, the energy-dependent treatment is beneficial to accurately draw the angular structure of neutrinos.

III. DEMONSTRATIONS

In this section we discuss the capability of our new method by demonstrating ELN-crossing searches using neutrino data of 1D and 2D CCSN simulations with full Boltzmann neutrino transport. We employ the most recent CCSN models of a 11.2 solar mass progenitor at a time snapshot of 250 ms after bounce. The detailed features of CCSN dynamics were discussed in our previous papers for 1D [103] and 2D [32]. In the raw neutrino data, we found no ELN crossings in the post-shock region for the 1D model. On the other hand, we found the crossings in the 2D data (we refer readers to N19 for the detailed analyses).

We first compute the energy-dependent zeroth and first angular moments of neutrinos from the distribution function of neutrinos (f) obtained from these simulations. We treat these moments as the input data for our method. The fluid data is also extracted from the simulations (see Fig. 1) to compute the reaction rates of neutrino-matter interactions (see Sec. II). In the following analyses, we use $G_{\rm in}$ and $G_{\rm out}$ to quantify the capability of our ELN-crossing search, which are defined as

$$G_{\rm in} = \int d\left(\frac{\varepsilon^3}{3}\right) f_{\rm in}(\varepsilon),$$
$$G_{\rm out} = \int d\left(\frac{\varepsilon^3}{3}\right) f_{\rm out}(\varepsilon), \tag{5}$$

where $f_{\rm out}$ denotes the distribution function f in the direction of $\mu = 1$. The energy integration on the right-hand side of Eq. (5) is carried out with units of MeV. We also compute the difference of G between ν_e and $\bar{\nu}_e$,

$$\Delta G = G_{\nu_e} - G_{\bar{\nu}_e}, \tag{6}$$

while we omit the indices of "in" and "out" in the expression. $\Delta G_{\rm in}$ and $\Delta G_{\rm out}$ are the most important variables in our method, since they are directly associated with ELN crossings. The former and latter represent the dominance of ν_e relative to $\bar{\nu}_e$ in the $\mu = -1$ (incoming) and $\mu = 1$ (outgoing) directions, respectively. In the case where the two variables have opposite sign, i.e.,

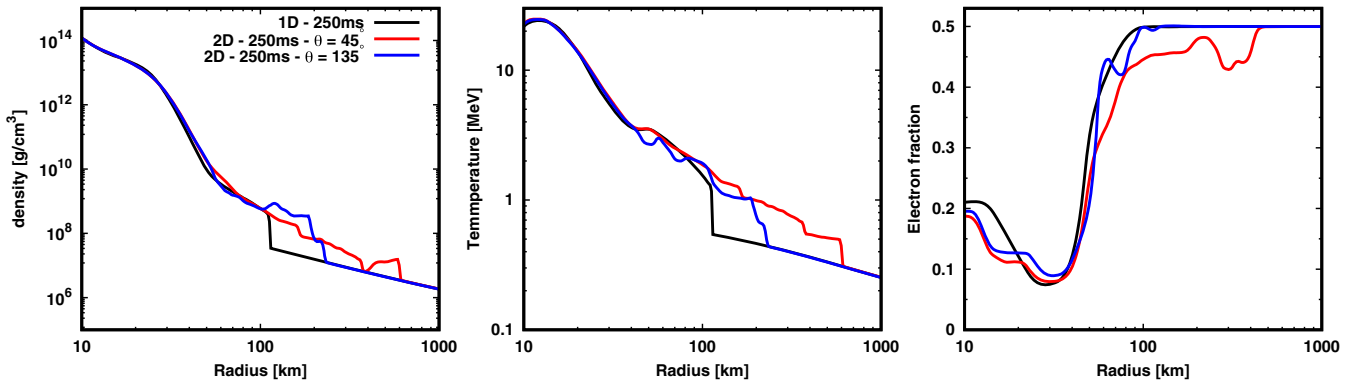

FIG. 1. From left to right, we show the radial profiles of the baryon mass density, matter temperature, and electron fraction, respectively, for CCSN models employed in this study. The detailed analyses can be seen in Refs. [103,32] for the 1D and 2D model, respectively. In this paper, we select the two radial rays ($\theta = 45°$ and 135°) in the 2D model as representative examples.

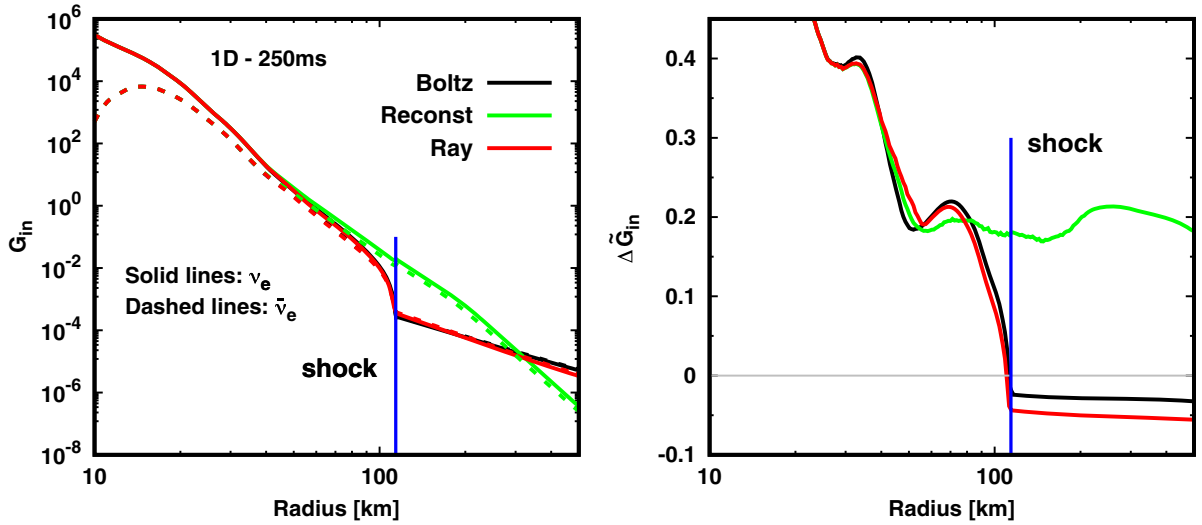

FIG. 2. Left: radial profile of $G_{\rm in}$ for the 1D CCSN model. Colors distinguish the difference in computing $G_{\rm in}$. The black line represents the result of $G_{\rm in}$ computed from f given by CCSN simulations with full Boltzmann neutrino transport. For the light-green one, $G_{\rm in}$ is computed from the reconstructed f from the zeroth and first moments using the method of N21. The red one corresponds to the result computed using our new method presented in this paper. The line type distinguishes the neutrino species; solid and dashed lines are for ν_e and $\bar{\nu}_e$, respectively. Right: the same as the left panel but for $\Delta\tilde{G}_{\rm in}$. It is $\Delta G_{\rm in}$ normalized by the summation of $G_{\rm in}$ over ν_e and $\bar{\nu}_e$. As a reference, the shock radius is displayed with a blue line in both panels. We also highlight $\Delta\tilde{G}_{\rm in} = 0$ by a gray line in the plot.

$\Delta G_{\rm out}\Delta G_{\rm in} < 0$, ν_e is dominant over $\bar{\nu}_e$ in either the $\mu = -1$ or 1 direction, while $\bar{\nu}_e$ overwhelms ν_e in the other direction, suggesting that ELN crossings occur in this case (see Sec. II for more details).

Figure 2 shows the radial profiles of $G_{\rm in}$ (left panel) and $\Delta\tilde{G}_{\rm in}$ (right panel) for the 1D CCSN model. $\Delta\tilde{G}_{\rm in}$ represents $\Delta G_{\rm in}$ normalized by the sum of $G_{\rm in}$ over ν_e and $\bar{\nu}_e$ at the same radius. This figure illustrates how much the ray-tracing treatment improves the computation of $G_{\rm in}$. In the left panel, $G_{\rm in}$ computed by the new method (red line) is almost identical to the original (black line), whereas the deviation is conspicuous at $\gtrsim$50 km for that computed from the reconstructed $f_{\rm in}$ from the zeroth and first moments (light-green line).

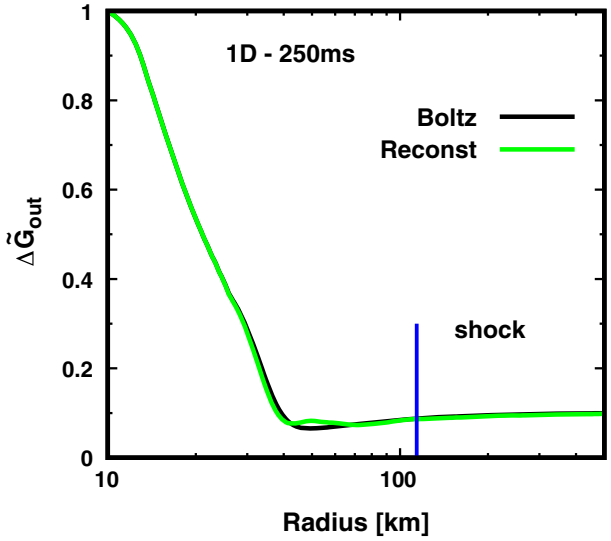

FIG. 3. Same as the right panel of Fig. 2 but for $G_{\rm out}$. We note that our new method adopts $f_{\rm out}$ reconstructed from the zeroth and first angular moments in the computation of $G_{\rm out}$; hence, we omit the red line in this figure. $\Delta\tilde{G}_{\rm out}$ denotes $\Delta G_{\rm out}$ normalized by the sum of $G_{\rm out}$ over ν_e and $\bar{\nu}_e$.

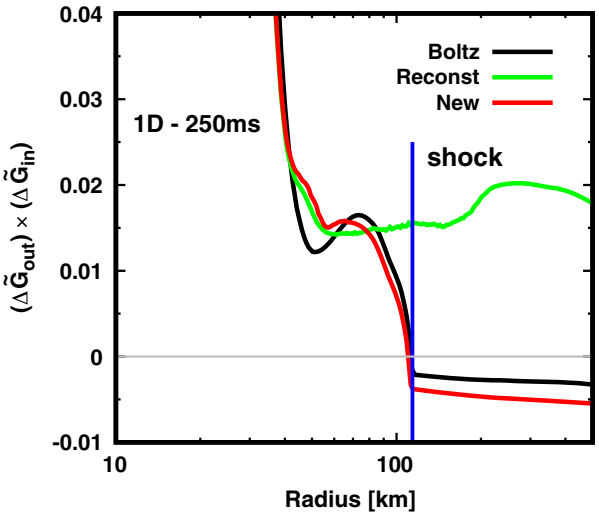

FIG. 4. Radial profile of $\Delta\tilde{G}_{\rm in} \times \Delta\tilde{G}_{\rm out}$ for the 1D model. The color coding is the same as in Fig. 2. We note that the title of the red line is changed from "Ray" to "New," since the previous title is misleading in this plot ($\tilde{G}_{\rm out}$ is computed from the reconstructed method of N21). See text for more details.

As shown in the left panel of Fig. 2, the difference of $G_{\rm in}$ between ν_e and $\bar{\nu}_e$ is subtle at $\gtrsim$50 km. This fact indicates that a high-fidelity computation of $G_{\rm in}$ is required to accurately reproduce the sign of $\Delta G_{\rm in}$, which is more clearly displayed in the right panel of Fig. 2. The difference of $G_{\rm in}$ between ν_e and $\bar{\nu}_e$ is a few percent of their summation (see black line in the right panel). Nevertheless, the new method reproduces the result of the original (compare red and black lines). On the other hand, the reconstructed counterpart (light-green line) generates qualitatively different $\Delta G_{\rm in}$; indeed, the sign of $\Delta G_{\rm in}$ becomes opposite from the original in the pre-shock region.

In Fig. 3 we compare the radial profile of $\Delta\tilde{G}_{\rm out}$ obtained by our new method to that of the original. Similar to $\Delta\tilde{G}_{\rm in}$, $\Delta\tilde{G}_{\rm out}$ denotes $\Delta G_{\rm out}$ normalized by the sum of $G_{\rm out}$ over ν_e and $\bar{\nu}_e$ at the same radius. In the computation of $G_{\rm out}$, we employ the reconstructed angular distribution from the zeroth and first angular moments following the method of N21. As mentioned already, the angular distributions of outgoing neutrinos can be well reconstructed without any extra prescriptions (see Sec. I). As expected, we confirm that $\Delta G_{\rm out}$ computed from the reconstructed distributions is very similar to that of the original, both of which are displayed in Fig. 3.

Both $\Delta G_{\rm in}$ and $\Delta G_{\rm out}$ computed by our new method show good agreement with the originals, indicating that their product, i.e., $\Delta G_{\rm out} \times \Delta G_{\rm in}$ is also captured accurately, which is displayed in Fig. 4. In the original profile (black line), the sign of the product is positive in the post-shock region, indicating that either ν_e or $\bar{\nu}_e$ is dominant in the entire neutrino flight direction,[9] i.e., there are no-ELN crossings in the region. On the contrary, the sign of the

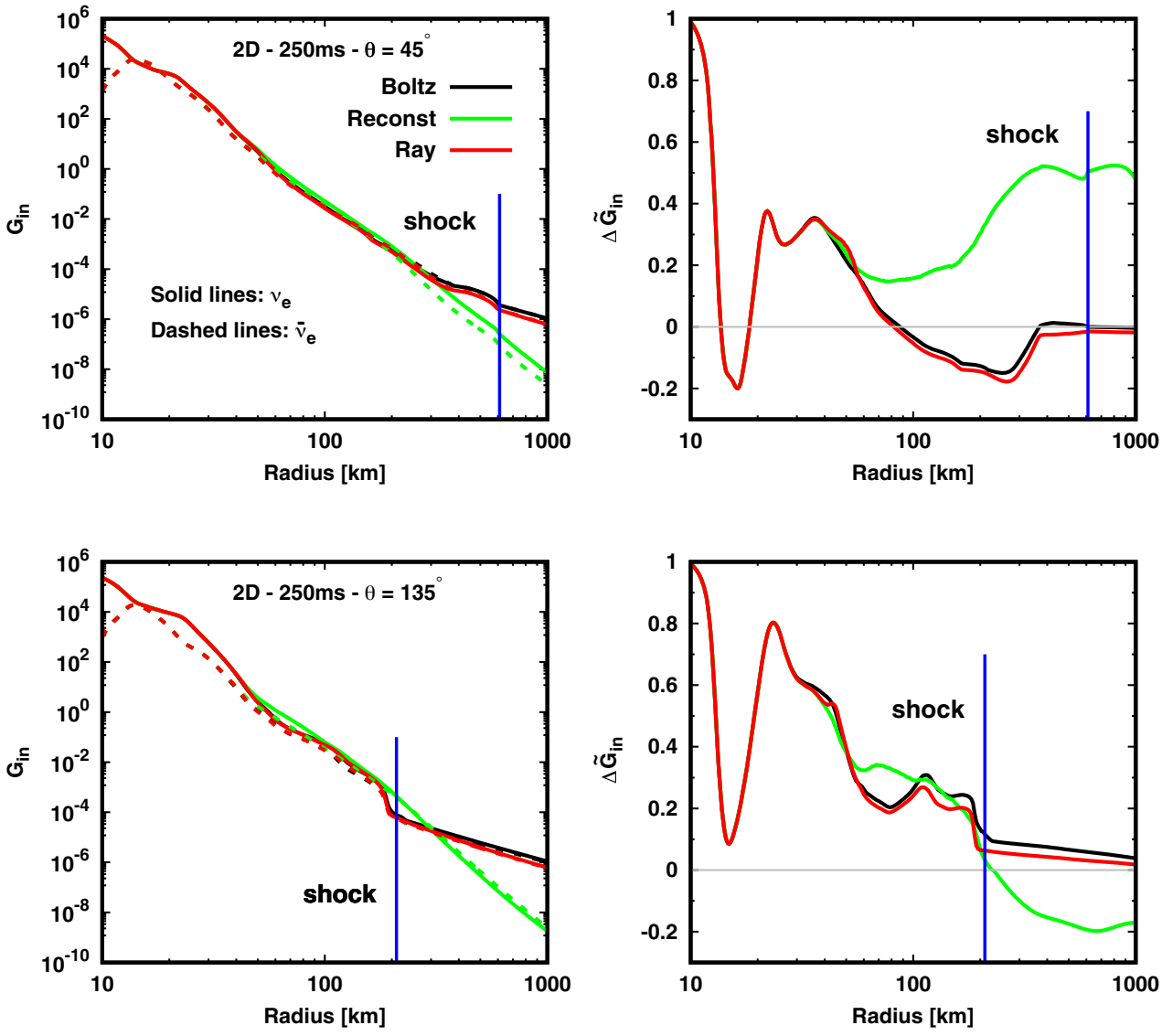

FIG. 5. Same as Fig. 2 but for the 2D CCSN model. The top and bottom panels show the results along the radial ray of $\theta = 45°$ and 135°, respectively.

product is negative in the pre-shock region; thus, the dominance of ν_e or $\bar{\nu}_e$ depends on the neutrino angle, indicating that ELN crossings appear. The key player to generate ELN crossings in pre-shock regions is a coherent scattering of heavy nuclei; the details of the physical mechanism were described in our previous paper [72]. Our new method detects the ELN crossing precisely, whereas one without the ray-tracing method does not. It should be emphasized that $\Delta G_{\rm out}$ is common for both methods, indicating that $\Delta G_{\rm in}$ is responsible for the difference. This is a strong evidence that our ray-tracing method qualitatively improves the accuracy of ELN-crossing searches.

We now turn our attention to the 2D model. It should be stressed that the spatial dimension does not change the procedure of our method, since we solve transport equations independently along each radial ray toward inward direction ($\mu = -1$). In the following analysis, we focus on two radial rays with $\theta = 45°$ and 135° in 2D space. We note that ELN crossings appear in the radial ray with $\theta = 45°$ in the original neutrino data with Boltzmann transport, whereas there are no ELN crossings at $\lesssim$1000 km in the ray with $\theta = 135°$ (see also Fig. 2 in N19). By applying our new method to search for ELN crossings along the two radial rays, we can assess the capability of our method in both cases with and without ELN crossings.

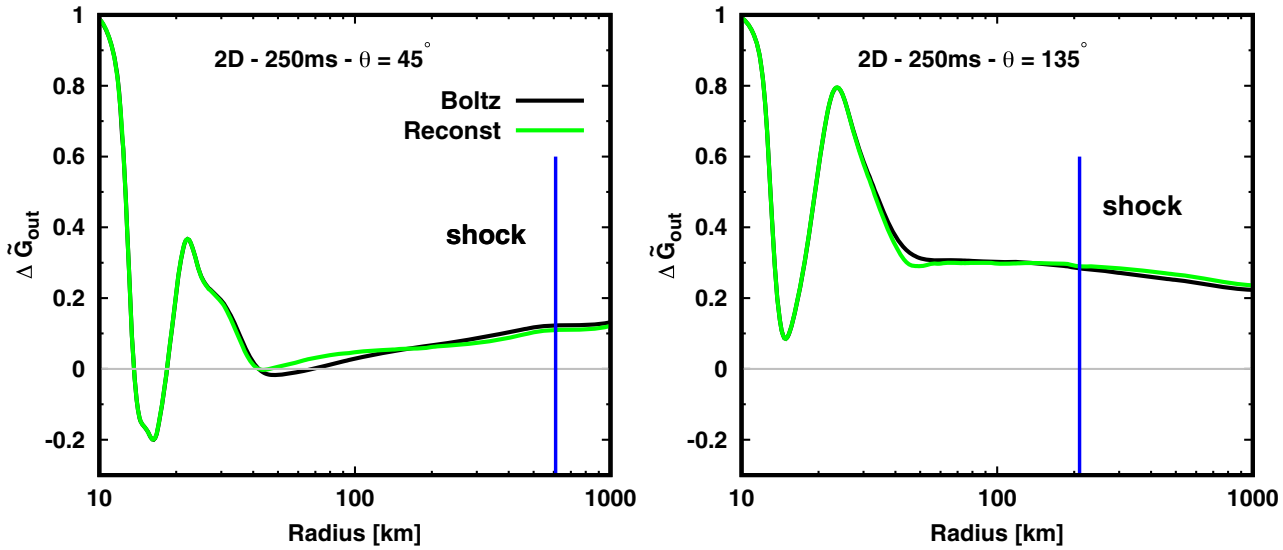

FIG. 6. Same as Fig. 3 but for the 2D CCSN model. The left and right panels display the result along the radial ray with $\theta = 45°$ and 135°, respectively.

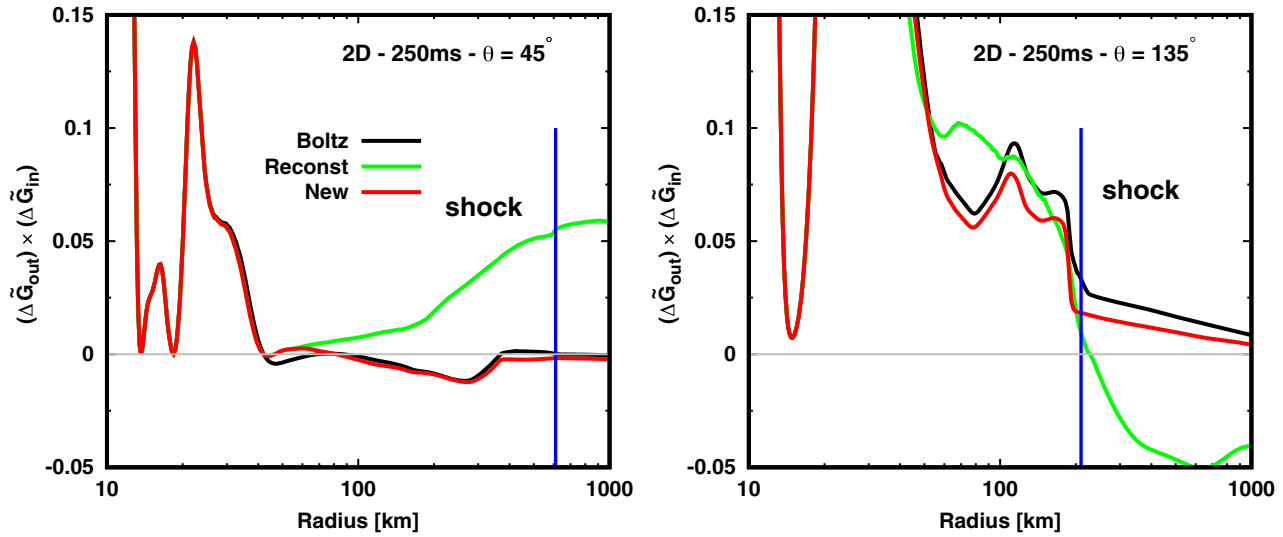

FIG. 7. Same as Fig. 4 but for the 2D CCSN model. The left and right panels display the result along the radial ray with $\theta = 45°$ and 135°, respectively.

Figure 5 portrays the radial distribution of $G_{\rm in}$ and $\Delta\tilde{G}_{\rm in}$ computed based on our new method (red line), reconstructed f from the zeroth and first moments (light-green line), and those given by Boltzmann neutrino transport (black line), the trend of which is essentially the same as that reported in our 1D model (see Fig. 2). We confirm that the new method substantially improves the computations of $G_{\rm in}$. We must note a caveat, however. At a radius of ∼500 km along the radial ray with $\theta = 45°$, our new method shows a different sign of $\Delta G_{\rm in}$ from that in the original (see top and right panels of Fig. 5). This is attributed to the fact that the difference of $G_{\rm in}$ between ν_e and $\bar{\nu}_e$ is so tiny. As a result, a small error in our method leads to misjudgments of the sign. This error may be reduced if we increase the level of approximations in our method. However, it would lead to an increase of the computational burden, which is undesirable for approximate ELN-crossing searches. To make more reliable judgements for such delicate ELN crossings, more complete treatments of neutrino transport, i.e., full Boltzmann neutrino transport would be indispensable.

In Fig. 6 we show the result of $\Delta\tilde{G}_{\rm out}$ as a function of radius. Let us emphasize again that $\Delta G_{\rm out}$ is obtained from the reconstructed f from the zeroth and first angular moments. This picture represents the good capability of our method. On the other hand, we again find a failure of capturing the sign of $\Delta G_{\rm out}$, at ∼50 km in the radial ray of $\theta = 45°$ (left panel of Fig. 6). Similar to the above argument, this error is attributed to the fact that the $G_{\rm out}$'s of ν_e and $\bar{\nu}_e$ are almost identical. Nevertheless, in most of the spatial regions, the basic features of $\Delta G_{\rm out}$ can be well captured by the new method.

The radial profile of $\Delta\tilde{G}_{\rm out} \times \Delta\tilde{G}_{\rm in}$ in the 2D model is displayed in Fig. 7. This illustrates that our new method provides the same judgement of ELN crossings as that made by Boltzmann neutrino transport along a radial ray with $\theta = 135°$. This is based on the fact that the ν_e number flux is substantially larger than that of $\bar{\nu}_e$ along the radial ray, which is due to coherent asymmetric neutrino emissions (see Ref. [32] for more details). As a result, there are no delicate competitions between ν_e and $\bar{\nu}_e$ for both inward and outward neutrino flight directions; hence, our method is capable of providing a robust diagnostics of ELN crossings. It should be stressed, however, that the judgment fails if we do not use a ray-tracing method. The low accuracy of reconstructing incoming neutrinos ($G_{\rm in}$) is mainly responsible for the misjudgment (see bottom panels of Fig. 5). In the radial ray with $\theta = 45°$, on the other hand, we find misjudgment even in the new method at ∼50 and ∼500 km. For the former and latter, this is due to the error of $G_{\rm out}$ and $G_{\rm in}$ in our method, respectively, the reason for which was already discussed. This result suggests that our new method is capable of detecting ELN crossings unless the crossing is so subtle (a few percent) in reality. We have to keep in mind the uncertainty and limitation when we apply our method for ELN-crossing searches.

[9]In this model, ν_e is dominant in the region.

IV. SUMMARY AND CONCLUSION

There is growing evidence that the appearance of ELN crossings in angular distributions of neutrinos is a precursor of fast-pairwise neutrino oscillation. This indication heightens the awareness of the importance of multiangle treatments of neutrino transport. However, the available CCSN models with full Boltzmann neutrino transport are still limited by their high computational burdens, which have inhibited the progress of the detailed analysis. On the other hand, there are many multi-D CCSN models with approximate neutrino transport, which covers the long-term post-bounce phase for various types of CCSN progenitors. This has motivated the community to develop surrogate methods to determine the occurrence of fast flavor conversions with limited information on neutrino radiation fields. The neutrino data is usually a few ranks of angular moments; hence, it is interesting to consider how we can utilize them in the analysis of flavor conversions.

Some previous works have tackled the issue. It turned out very recently, however, that they are not capable of identifying the occurrence of fast flavor conversions in the region of forward-peaked angular distributions. The source of the problem is that the low angular moments are insensitive to the incoming neutrinos in such regions. In this paper, we proposed to use a ray-tracing method to compensate for the shortage. In this method, we determined the ELN at $\mu = 1$ (outgoing neutrinos) using the reconstructed angular distributions of neutrinos from the zeroth and first moments using the method of N21. On the other hand, the determination of ELN at $\mu = -1$ is complemented by the ray-tracing method. In Sec. III, we assessed the capability of our method by making a detailed comparison to results of full Boltzmann neutrino transport in 1D and 2D. We demonstrated that our new method substantially improves the accuracy of ELN-crossing searches. Unless the crossing is very subtle (a few percent of the sum of the occupation numbers of ν_e and $\bar{\nu}_e$), our method is capable of making accurate judgements of ELN crossings.

We next applied our new method presented in this paper to multi-D CCSN models with multigroup two-moment neutrino transport. The results will be discussed in a separate paper.

ACKNOWLEDGMENTS

We acknowledge conversations with Sherwood Richers, Sam Flynn, Nicole Ford, Evan Grohs, Jim Kneller, Gail McLaughlin, Don Willcox, Taiki Morinaga, Eirik Endeve, and Adam Burrows. H. N. acknowledges support from the

U.S. Department of Energy Office of Science and the Office of Advanced Scientific Computing Research via the Scientific Discovery through Advanced Computing (SciDAC4) program and Grant No. DE-SC0018297 (subaward 00009650). The numerical computations of our CCSN models were performed on the K computer at the RIKEN under HPCI Strategic Program of Japanese MEXT (Project ID: hpci 160071, 160211, 170230, 170031, 170304, hp180179, hp180111, and hp180239). L. J. acknowledges support provided by NASA through the NASA Hubble Fellowship Grant No. HST-HF2-51461.001-A awarded by the Space Telescope Science Institute, which is operated by the Association of Universities for Research in Astronomy, Incorporated, under NASA Contract No. NAS5-26555.

[1] H.-T. Janka, Neutrino-driven explosions, in *Handbook of Supernovae* (Springer International Publishing, AG, 2017), p. 1095, ISBN 978-3-319-21845-8.
[2] B. Müller, Hydrodynamics of core-collapse supernovae and their progenitors, Living Rev. Comput. Astrophys. **6**, 3 (2020).
[3] A. Mezzacappa, E. Endeve, O. E. B. Messer, and S. W. Bruenn, Physical, numerical, and computational challenges of modeling neutrino transport in core-collapse supernovae, Living Rev. Comput. Astrophys. **6**, 4 (2020).
[4] A. Burrows and D. Vartanyan, Core-collapse supernova explosion theory, Nature (London) **589**, 29 (2021).
[5] Y. Z. Qian and S. E. Woosley, Nucleosynthesis in neutrino-driven winds. I. The physical conditions, Astrophys. J. **471**, 331 (1996).
[6] C. J. Horowitz and G. Li, Nucleosynthesis in Supernovae, Phys. Rev. Lett. **82**, 5198 (1999).
[7] L. F. Roberts, S. E. Woosley, and R. D. Hoffman, Integrated nucleosynthesis in neutrino-driven winds, Astrophys. J. **722**, 954 (2010).
[8] Y. Yamamoto, S.-i. Fujimoto, H. Nagakura, and S. Yamada, Post-shock-revival evolution in the neutrino-heating mechanism of core-collapse supernovae, Astrophys. J. **771**, 27 (2013).
[9] G. Martínez-Pinedo, T. Fischer, and L. Huther, Supernova neutrinos and nucleosynthesis, J. Phys. G **41**, 044008 (2014).
[10] M. Eichler, K. Nakamura, T. Takiwaki, T. Kuroda, K. Kotake, M. Hempel, R. Cabezón, M. Liebendörfer, and F. K. Thielemann, Nucleosynthesis in 2D core-collapse supernovae of 11.2 and 17.0 M progenitors: implications for Mo and Ru production, J. Phys. G **45**, 014001 (2018).
[11] S. Wanajo, B. Müller, H.-T. Janka, and A. Heger, Nucleosynthesis in the innermost ejecta of neutrino-driven supernova explosions in two dimensions, Astrophys. J. **852**, 40 (2018).
[12] S.-i. Fujimoto and H. Nagakura, The impact of asymmetric neutrino emissions on nucleosynthesis in core-collapse supernovae, Mon. Not. R. Astron. Soc. **488**, L114 (2019).
[13] A. Sieverding, B. Müller, and Y. Z. Qian, Nucleosynthesis of an 11.8 M supernova with 3D Simulation of the inner ejecta: overall yields and implications for short-lived radionuclides in the early solar system, Astrophys. J. **904**, 163 (2020).
[14] S.-i. Fujimoto and H. Nagakura, The impact of asymmetric neutrino emissions on nucleosynthesis in core-collapse supernovae II—Progenitor dependences, Mon. Not. R. Astron. Soc. **502**, 2319 (2021).
[15] I. Tamborra, F. Hanke, B. Müller, H.-T. Janka, and G. Raffelt, Neutrino Signature of Supernova Hydrodynamical Instabilities in Three Dimensions, Phys. Rev. Lett. **111**, 121104 (2013).
[16] K. Nakazato, K. Sumiyoshi, H. Suzuki, T. Totani, H. Umeda, and S. Yamada, Supernova neutrino light curves and spectra for various progenitor stars: From core collapse to proto-neutron star cooling, Astrophys. J. Suppl. Ser. **205**, 2 (2013).
[17] K. Nakamura, S. Horiuchi, M. Tanaka, K. Hayama, T. Takiwaki, and K. Kotake, Multimessenger signals of long-term core-collapse supernova simulations: Synergetic observation strategies, Mon. Not. R. Astron. Soc. **461**, 3296 (2016).
[18] B. Müller, Neutrino emission as diagnostics of core-collapse supernovae, Annu. Rev. Nucl. Part. Sci. **69**, 253 (2019).
[19] Z. Lin, C. Lunardini, M. Zanolin, K. Kotake, and C. Richardson, Detectability of SASI activity in supernova neutrino signals, Phys. Rev. D **101**, 123028 (2020).
[20] M. L. Warren, S. M. Couch, E. P. O'Connor, and V. Morozova, Constraining properties of the next nearby core-collapse supernova with multimessenger signals, Astrophys. J. **898**, 139 (2020).
[21] H. Nagakura, A. Burrows, D. Vartanyan, and D. Radice, Core-collapse supernova neutrino emission and detection informed by state-of-the-art three-dimensional numerical models, Mon. Not. R. Astron. Soc. **500**, 696 (2021).
[22] H. Nagakura, A. Burrows, and D. Vartanyan, Supernova neutrino signals based on long-term axisymmetric simulations, Mon. Not. R. Astron. Soc. **506**, 1462 (2021).
[23] Y. Suwa, A. Harada, K. Nakazato, and K. Sumiyoshi, Analytic solutions for neutrino-light curves of core-collapse supernovae, Prog. Theor. Exp. Phys. **2021**, 013E01 (2021).
[24] A. Mirizzi, I. Tamborra, H. Th. Janka, N. Saviano, K. Scholberg, R. Bollig, L. Hüdepohl, and S. Chakraborty, Supernova neutrinos: Production, oscillations and detection, Nuovo Cimento Riv. Ser. **39**, 1 (2016).

[25] S. Horiuchi and J. P. Kneller, What can be learned from a future supernova neutrino detection?, J. Phys. G **45**, 043002 (2018).
[26] B. Dasgupta and J. F. Beacom, Reconstruction of supernova ν_μ, ν_τ, anti-ν_μ, and anti-ν_τ neutrino spectra at scintillator detectors, Phys. Rev. D **83**, 113006 (2011).
[27] H.-L. Li, X. Huang, Y.-F. Li, L.-J. Wen, and S. Zhou, Model-independent approach to the reconstruction of multiflavor supernova neutrino energy spectra, Phys. Rev. D **99**, 123009 (2019).
[28] H. Nagakura, Retrieval of energy spectra for all flavours of neutrinos from core-collapse supernova with multiple detectors, Mon. Not. R. Astron. Soc. **500**, 319 (2021).
[29] A. S. Dighe and A. Yu. Smirnov, Identifying the neutrino mass spectrum from a supernova neutrino burst, Phys. Rev. D **62**, 033007 (2000).
[30] H. Nagakura, W. Iwakami, S. Furusawa, H. Okawa, A. Harada, K. Sumiyoshi, S. Yamada, H. Matsufuru, and A. Imakura, Simulations of core-collapse supernovae in spatial axisymmetry with full boltzmann neutrino transport, Astrophys. J. **854**, 136 (2018).
[31] A. Harada, H. Nagakura, W. Iwakami, H. Okawa, S. Furusawa, H. Matsufuru, K. Sumiyoshi, and S. Yamada, On the neutrino distributions in phase space for the rotating core-collapse supernova simulated with a Boltzmann-neutrino-radiation-hydrodynamics code, Astrophys. J. **872**, 181 (2019).
[32] H. Nagakura, K. Sumiyoshi, and S. Yamada, Possible early linear acceleration of proto-neutron stars via asymmetric neutrino emission in core-collapse supernovae, Astrophys. J. Lett. **880**, L28 (2019).
[33] W. Iwakami, H. Okawa, H. Nagakura, A. Harada, S. Furusawa, K. Sumiyoshi, H. Matsufuru, and S. Yamada, Simulations of the early postbounce phase of core-collapse supernovae in three-dimensional space with full Boltzmann neutrino transport, Astrophys. J. **903**, 82 (2020).
[34] H. Duan, G. M. Fuller, and Y.-Z. Qian, Collective neutrino oscillations, Annu. Rev. Nucl. Part. Sci. **60**, 569 (2010).
[35] G. Raffelt, G. Sigl, and L. Stodolsky, Non-Abelian Boltzmann Equation for Mixing and Decoherence, Phys. Rev. Lett. **70**, 2363 (1993).
[36] M. Sirera and A. Pérez, Relativistic Wigner function approach to neutrino propagation in matter, Phys. Rev. D **59**, 125011 (1999).
[37] S. Yamada, Boltzmann equations for neutrinos with flavor mixings, Phys. Rev. D **62**, 093026 (2000).
[38] C. Volpe, D. Väänänen, and C. Espinoza, Extended evolution equations for neutrino propagation in astrophysical and cosmological environments, Phys. Rev. D **87**, 113010 (2013).
[39] A. Vlasenko, G. M. Fuller, and V. Cirigliano, Neutrino quantum kinetics, Phys. Rev. D **89**, 105004 (2014).
[40] V. Cirigliano, G. M. Fuller, and A. Vlasenko, A new spin on neutrino quantum kinetics, Phys. Lett. B **747**, 27 (2015).
[41] C. Volpe, Neutrino quantum kinetic equations, Int. J. Mod. Phys. E **24**, 1541009 (2015).
[42] D. N. Blaschke and V. Cirigliano, Neutrino quantum kinetic equations: The collision term, Phys. Rev. D **94**, 033009 (2016).
[43] S. Abbar and M. C. Volpe, On fast neutrino flavor conversion modes in the nonlinear regime, Phys. Lett. B **790**, 545 (2019).
[44] S. A. Richers, G. C. McLaughlin, J. P. Kneller, and A. Vlasenko, Neutrino quantum kinetics in compact objects, Phys. Rev. D **99**, 123014 (2019).
[45] J. D. Martin, S. Abbar, and H. Duan, Nonlinear flavor development of a two-dimensional neutrino gas, Phys. Rev. D **100**, 023016 (2019).
[46] F. Capozzi, B. Dasgupta, A. Mirizzi, M. Sen, and G. Sigl, Collisional Triggering of Fast Flavor Conversions of Supernova Neutrinos, Phys. Rev. Lett. **122**, 091101 (2019).
[47] H. Sasaki, T. Takiwaki, S. Kawagoe, S. Horiuchi, and K. Ishidoshiro, Detectability of collective neutrino oscillation signatures in the supernova explosion of a 8.8 M star, Phys. Rev. D **101**, 063027 (2020).
[48] I. Tamborra and S. Shalgar, New developments in flavor evolution of a dense neutrino gas, arXiv:2011.01948.
[49] S. Shalgar, I. Padilla-Gay, and I. Tamborra, Neutrino propagation hinders fast pairwise flavor conversions, J. Cosmol. Astropart. Phys. 06 (2020) 048.
[50] S. Bhattacharyya and B. Dasgupta, Fast Flavor Depolarization of Supernova Neutrinos, Phys. Rev. Lett. **126**, 061302 (2021).
[51] J. D. Martin, J. Carlson, V. Cirigliano, and H. Duan, Fast flavor oscillations in dense neutrino media with collisions, Phys. Rev. D **103**, 063001 (2021).
[52] S. Richers, D. E. Willcox, N. M. Ford, and A. Myers, Particle-in-cell simulation of the neutrino fast flavor instability, Phys. Rev. D **103**, 083013 (2021).
[53] M. Zaizen and T. Morinaga, Nonlinear evolution of fast neutrino flavor conversion in the preshock region of core-collapse supernovae, arXiv:2104.10532.
[54] S. Shalgar and I. Tamborra, Dispelling a myth on dense neutrino media: Fast pairwise conversions depend on energy, J. Cosmol. Astropart. Phys. 01 (2021) 014.
[55] S. Shalgar and I. Tamborra, The three flavor revolution in fast pairwise neutrino conversion, Phys. Rev. D **104**, 023011 (2021).
[56] R. F. Sawyer, Speed-up of neutrino transformations in a supernova environment, Phys. Rev. D **72**, 045003 (2005).
[57] R. Bollig, H. T. Janka, A. Lohs, G. Martínez-Pinedo, C. J. Horowitz, and T. Melson, Muon Creation in Supernova Matter Facilitates Neutrino-Driven Explosions, Phys. Rev. Lett. **119**, 242702 (2017).
[58] T. Fischer, G. Guo, G. Martínez-Pinedo, M. Liebendörfer, and A. Mezzacappa, Muonization of supernova matter, Phys. Rev. D **102**, 123001 (2020).
[59] G. Guo, G. Martínez-Pinedo, A. Lohs, and T. Fischer, Charged-current muonic reactions in core-collapse supernovae, Phys. Rev. D **102**, 023037 (2020).
[60] F. Capozzi, M. Chakraborty, S. Chakraborty, and M. Sen, Mu-Tau Neutrinos: Influencing Fast Flavor Conversions in Supernovae, Phys. Rev. Lett. **125**, 251801 (2020).
[61] F. Capozzi, S. Abbar, R. Bollig, and H. T. Janka, Fast neutrino flavor conversions in one-dimensional core-collapse supernova models with and without muon creation, Phys. Rev. D **103**, 063013 (2021).

[62] I. Izaguirre, G. Raffelt, and I. Tamborra, Fast Pairwise Conversion of Supernova Neutrinos: A Dispersion Relation Approach, Phys. Rev. Lett. **118**, 021101 (2017).
[63] B. Dasgupta, A. Mirizzi, and M. Sen, Fast neutrino flavor conversions near the supernova core with realistic flavor-dependent angular distributions, J. Cosmol. Astropart. Phys. 02 (2017) 019.
[64] S. Shalgar and I. Tamborra, Change of direction in pairwise neutrino conversion physics: The effect of collisions, Phys. Rev. D **103**, 063002 (2021).
[65] S. Bhattacharyya and B. Dasgupta, Fast flavor oscillations of astrophysical neutrinos with $1, 2, \ldots, \infty$ crossings, J. Cosmol. Astropart. Phys. 07 (2021) 023.
[66] T. Morinaga, Fast neutrino flavor instability and neutrino flavor lepton number crossings, arXiv:2103.15267.
[67] S. Abbar, H. Duan, K. Sumiyoshi, T. Takiwaki, and M. C. Volpe, On the occurrence of fast neutrino flavor conversions in multidimensional supernova models, Phys. Rev. D **100**, 043004 (2019).
[68] M. D. Azari, S. Yamada, T. Morinaga, W. Iwakami, H. Okawa, H. Nagakura, and K. Sumiyoshi, Linear analysis of fast-pairwise collective neutrino oscillations in core-collapse supernovae based on the results of Boltzmann simulations, Phys. Rev. D **99**, 103011 (2019).
[69] H. Nagakura, T. Morinaga, C. Kato, and S. Yamada, Fast-pairwise collective neutrino oscillations associated with asymmetric neutrino emissions in core-collapse supernovae, Astrophys. J. **886**, 139 (2019).
[70] S. Abbar, H. Duan, K. Sumiyoshi, T. Takiwaki, and M. C. Volpe, Fast neutrino flavor conversion modes in multidimensional core-collapse supernova models: The role of the asymmetric neutrino distributions, Phys. Rev. D **101**, 043016 (2020).
[71] M. D. Azari, S. Yamada, T. Morinaga, H. Nagakura, S. Furusawa, A. Harada, H. Okawa, W. Iwakami, and K. Sumiyoshi, Fast collective neutrino oscillations inside the neutrino sphere in core-collapse supernovae, Phys. Rev. D **101**, 023018 (2020).
[72] T. Morinaga, H. Nagakura, C. Kato, and S. Yamada, Fast neutrino-flavor conversion in the preshock region of core-collapse supernovae, Phys. Rev. Research **2**, 012046 (2020).
[73] J. L. Anderson and E. A. Spiegel, The moment method in relativistic radiative transfer, Astrophys. J. **171**, 127 (1972).
[74] K. S. Thorne, Relativistic radiative transfer—Moment formalisms, Mon. Not. R. Astron. Soc. **194**, 439 (1981).
[75] O. Just, M. Obergaulinger, and H. T. Janka, A new multidimensional, energy-dependent two-moment transport code for neutrino-hydrodynamics, Mon. Not. R. Astron. Soc. **453**, 3387 (2015).
[76] F. Foucart, E. O'Connor, L. Roberts, M. D. Duez, R. Haas, L. E. Kidder, C. D. Ott, H. P. Pfeiffer, M. A. Scheel, and B. Szilagyi, Post-merger evolution of a neutron star-black hole binary with neutrino transport, Phys. Rev. D **91**, 124021 (2015).
[77] M. Shibata, K. Kiuchi, Y. Sekiguchi, and Y. Suwa, Truncated moment formalism for radiation hydrodynamics in numerical relativity, Prog. Theor. Phys. **125**, 1255 (2011).
[78] M. A. Skinner, J. C. Dolence, A. Burrows, D. Radice, and D. Vartanyan, FORNAX: A flexible code for multiphysics astrophysical simulations, Astrophys. J. Suppl. Ser. **241**, 7 (2019).
[79] M. P. Laiu, E. Endeve, R. Chu, J. A. Harris, and O. E. B. Messer, A DG-IMEX method for two-moment neutrino transport: Nonlinear solvers for neutrino-matter coupling, Astrophys. J. Suppl. Ser. **253**, 52 (2021).
[80] L. F. Roberts, C. D. Ott, R. Haas, E. P. O'Connor, P. Diener, and E. Schnetter, General-relativistic three-dimensional multi-group neutrino radiation-hydrodynamics simulations of core-collapse supernovae, Astrophys. J. **831**, 98 (2016).
[81] T. Kuroda, T. Takiwaki, and K. Kotake, A new multi-energy neutrino radiation-hydrodynamics code in full general relativity and its application to the gravitational collapse of massive stars, Astrophys. J. Suppl. Ser. **222**, 20 (2016).
[82] E. P. O'Connor and S. M. Couch, Exploring fundamentally three-dimensional phenomena in high-fidelity simulations of core-collapse supernovae, Astrophys. J. **865**, 81 (2018).
[83] T. Kuroda, K. Kotake, T. Takiwaki, and F.-K. Thielemann, A full general relativistic neutrino radiation-hydrodynamics simulation of a collapsing very massive star and the formation of a black hole, Mon. Not. R. Astron. Soc. **477**, L80 (2018).
[84] H. Nagakura, A. Burrows, D. Radice, and D. Vartanyan, Towards an understanding of the resolution dependence of Core-Collapse Supernova simulations, Mon. Not. R. Astron. Soc. **490**, 4622 (2019).
[85] D. Vartanyan, A. Burrows, D. Radice, M. A. Skinner, and J. Dolence, A successful 3D core-collapse supernova explosion model, Mon. Not. R. Astron. Soc. **482**, 351 (2019).
[86] R. Glas, O. Just, H. T. Janka, and M. Obergaulinger, Three-dimensional core-collapse supernova simulations with multidimensional neutrino transport compared to the ray-by-ray-plus approximation, Astrophys. J. **873**, 45 (2019).
[87] A. S. Schneider, L. F. Roberts, C. D. Ott, and E. O'Connor, Equation of state effects in the core collapse of a 20-M star, Phys. Rev. C **100**, 055802 (2019).
[88] A. Burrows, D. Radice, D. Vartanyan, H. Nagakura, M. A. Skinner, and J. C. Dolence, The overarching framework of core-collapse supernova explosions as revealed by 3D FORNAX simulations, Mon. Not. R. Astron. Soc. **491**, 2715 (2020).
[89] H. Nagakura, A. Burrows, D. Radice, and D. Vartanyan, A systematic study of proto-neutron star convection in three-dimensional core-collapse supernova simulations, Mon. Not. R. Astron. Soc. **492**, 5764 (2020).
[90] J. Powell and B. Müller, Three-dimensional core-collapse supernova simulations of massive and rotating progenitors, Mon. Not. R. Astron. Soc. **494**, 4665 (2020).
[91] B. Müller and V. Varma, A 3D simulation of a neutrino-driven supernova explosion aided by convection and magnetic fields, Mon. Not. R. Astron. Soc. **498**, L109 (2020).
[92] R. Bollig, N. Yadav, D. Kresse, H. Th. Janka, B. Mueller, and A. Heger, Self-consistent 3D supernova models from -7 minutes to $+7$ seconds: A 1-bethe explosion of a $\sim$19 solar-mass progenitor, Astrophys. J. **915**, 28 (2021).

[93] B. Dasgupta, A. Mirizzi, and M. Sen, Simple method of diagnosing fast flavor conversions of supernova neutrinos, Phys. Rev. D **98**, 103001 (2018).

[94] R. Glas, H. T. Janka, F. Capozzi, M. Sen, B. Dasgupta, A. Mirizzi, and G. Sigl, Fast neutrino flavor instability in the neutron-star convection layer of three-dimensional supernova models, Phys. Rev. D **101**, 063001 (2020).

[95] S. Abbar, Searching for fast neutrino flavor conversion modes in core-collapse supernova simulations, J. Cosmol. Astropart. Phys. 05 (2020) 027.

[96] S. Abbar, F. Capozzi, R. Glas, H. T. Janka, and I. Tamborra, On the characteristics of fast neutrino flavor instabilities in three-dimensional core-collapse supernova models, Phys. Rev. D **103**, 063033 (2021).

[97] E. M. Murchikova, E. Abdikamalov, and T. Urbatsch, Analytic closures for M1 neutrino transport, Mon. Not. R. Astron. Soc. **469**, 1725 (2017).

[98] L. Johns and H. Nagakura, Fast flavor instabilities and the search for neutrino angular crossings, Phys. Rev. D **103**, 123012 (2021).

[99] H. Nagakura and L. Johns, Constructing angular distributions of neutrinos in core collapse supernova from zero-th and first moments calibrated by full Boltzmann neutrino transport, Phys. Rev. D **103**, 123025 (2021).

[100] S. Richers, H. Nagakura, C. D. Ott, J. Dolence, K. Sumiyoshi, and S. Yamada, A detailed comparison of multidimensional Boltzmann neutrino transport methods in core-collapse supernovae, Astrophys. J. **847**, 133 (2017).

[101] S. W. Bruenn, Stellar core collapse—Numerical model and infall epoch, Astrophys. J. Suppl. Ser. **58**, 771 (1985).

[102] H. Nagakura, K. Sumiyoshi, and S. Yamada, Three-dimensional Boltzmann hydro code for core collapse in massive stars. i. Special relativistic treatments, Astrophys. J. Suppl. Ser. **214**, 16 (2014).

[103] H. Nagakura, S. Furusawa, H. Togashi, S. Richers, K. Sumiyoshi, and S. Yamada, Comparing treatments of weak reactions with nuclei in simulations of core-collapse supernovae, Astrophys. J. Suppl. Ser. **240**, 38 (2019).